Deuterium-MAS NMR Spectroscopy on Oriented Membrane Proteins: Applications to Photointermediates of Bacteriorhodopsin

Clemens Glaubitz,* Ian J. Burnett, Gerhard Gröbner, A. James Mason, and Anthony Watts

Contribution from the Department of Biochemistry, Biomembrane Structure Unit, University of Oxford, South Parks Road, Oxford OX1 3QU, Great Britain

Received February 4, 1999. Revised Manuscript Received April 16, 1999

Abstract: We present the first application of MAOSS (magic angle oriented sample spinning) NMR spectroscopy to a large membrane protein. This new solid-state NMR approach is used to study the orientation of the deuterated methyl group in [18-CD_3]-retinal in oriented bacteriorhodopsin in both the photocycle ground state (bR_{568}) and in the photo intermediate state M_{412}. Deuterium MAS spectra consist of a set of narrow spinning sidebands if the sample spinning rate does not exceed the anisotropy of the quadrupole interaction. In ordered systems, such as proteins in oriented membranes, each sideband intensity is orientationally dependent. The observed MAS sideband pattern is modulated in a highly sensitive way by changes in the molecular orientation of the CD_3 group during the transition from all-*trans*- to 13-*cis*-retinal upon photoactivation. The significant improvement in spectral sensitivity and resolution, compared to static NMR on oriented samples, allows a reliable and precise data analysis even from lower spin concentrations and has more general consequences for studying oriented membrane proteins by NMR. MAOSS NMR is shown to be a feasible method for the accurate determination of local molecular orientations in large molecular systems which are currently a challenge for crystallography.

Introduction

Membrane proteins, which represent ∼30−50% of the information encoded by known genomes,[1] mediate some of the most important functions carried out by the cell. These functions, such as signal transduction across the membrane bilayer, secretion of toxins, transport of ions and nutrients, make them important potential drug targets.[2] Knowledge of their structure is of central importance for understanding their functional mechanisms. However, structure determinations are still a technological challenge, since membrane proteins are not well-suited for study by the principal high-resolution structural methods (X-ray diffraction, liquid-state NMR). The lipids required for structure and function of membrane proteins interfere with crystallization or rapid reorientation in solution. As a result, our knowledge of membrane protein structure lags far behind that of soluble proteins. One approach, which has undergone a remarkable development in recent years, uses solid-state NMR spectroscopy which does not require crystals, allows use of a bilayer environment, and does not depend on short motional correlation times.[2−4]

To establish a molecular model for a membrane protein, it is necessary to acquire information about the secondary protein structure and about the orientation of the protein within the anisotropic membrane environment.[5] These data can be provided by solid-state NMR, if a sufficiently high spectral resolution for the nuclei of interest (^2H, ^{13}C, ^{15}N) is achieved, which is necessary to be able to utilize isotropic and anisotropic chemical shifts, as well as dipolar, quadrupole, and *J*-couplings.[6]

In principle, good spectral resolution can be obtained by using the anisotropic, two-dimensional character of membranes to prepare macroscopically ordered samples with well-oriented lipids and proteins, either by aligning them in bilayers on glass disks[5,7] or by using bicelles.[8−10] Since the signal frequency observed from a second rank tensor interaction depends on its orientation Ω_{PL} with respect to the laboratory frame, sharp resonance lines would be observed if all tensors would have the same orientation with respect to the magnetic field B_0. This effect has been used extensively for studying macroscopically aligned membranes, by utilizing the orientationally dependent anisotropies of either quadrupole interaction (^2H), of chemical shielding tensors (^{13}C, ^{15}N, ^{31}P), and dipolar couplings ($^{15}N-^1H$). For example, the orientation of ^2H-labeled chromophores in bacteriorhodopsin[11,12] and bovine rhodopsin[13] have been determined, as well as the orientation and structure of gramicidin[14] and other helical peptides.[15] The possibility of obtaining

* Corresponding author.

(1) Arkin, I. T.; Brunger, A. T.; Engelman, D. M. *Proteins* **1997**, *28*, 465−466.
(2) Watts, A.; Burnett, I. J.; Glaubitz, C.; Gröbner, G.; Middleton, D. A.; Spooner, P. J. R.; Williamson, P. T. F. *Eur. Biophys. J.* **1998**, *28*, 84−90.
(3) Opella, S. J. *Nat. Struct. Biol.* **1997**, *4*, 845−848.
(4) Smith, S. O.; Aschheim, K.; Groesbeek, M. *Q. Rev. Biophys.* **1996**, *29*, 395−449.
(5) Cross, T. A.; Opella, S. J. *Curr. Opin. Struct. Biol.* **1994**, *4*, 574−581.
(6) Tycko, R. *J. Biomol. NMR* **1996**, *8*, 239−251.
(7) Gröbner, G.; Taylor, A.; Williamson, P. T. F.; Choi, G.; Glaubitz, C.; Watts, J. A.; de Grip, W. J.; Watts, A. *Anal. Biochem.* **1997**, *254*, 132−138.
(8) Sanders, C. R.; Hare, B. J.; Howerd, K.; Prestegard, J. H. *Prog. Nucl. Magn. Reson. Spectrosc.* **1993**, *26*, 421−444.
(9) Prosser, S. R.; Hunt, S. A.; Dinatale, J. T.; Vold, R. R. *J. Am. Chem. Soc.* **1996**, *118*, 269−270.
(10) Howard, K. P.; Opella, S. J. *J. Magn. Res.* **1996**, *112*, 91−94.
(11) Ulrich, A. S.; Wallat, I.; Heyn, M. P.; Watts, A. *Nat. Struct. Biol.* **1995**, *2*, 190−192.
(12) Moltke, S.; Nevzorov, A. A.; Sakai, N.; Wallat, I.; Job, C.; Nakanishi, K.; Heyn, M. P.; Brown, M. F. *Biochemistry* **1998**, *37*, 11821−11835.
(13) Gröbner, G.; Choi, G.; Burnett, I. J.; Glaubitz, C.; Verdegem, P. J. M.; Lugtenburg, J.; Watts, A. *FEBS Lett.* **1998**, *422*, 201−204.

10.1021/ja990350p CCC: $18.00
Published on Web 06/05/1999

completely resolved ^{15}N spectra of fully labeled peptides was recently shown for the fd-coat protein.[16] However, two potential drawbacks exist with these approaches. Resonance assignment in multiple or uniformly labeled proteins can cause problems since each resonance depends on tensor size and orientation, which would make assuming a molecular geometry necessary prior to full spectral assignment. Also, deviations from perfect alignment, which are common for large proteins such as rhodopsin in bilayers, make a significant contribution to the linewidth, making this static NMR approach less straightforward.[13]

In contrast to static NMR on oriented membranes, magic angle sample spinning NMR spectroscopy provides well-resolved spectra by projecting all anisotropic interactions causing linebroadening onto the MAS rotor long axis where they collapse at the magic angle.[17] For rapid spinning, only the isotropic chemical shift is retained, resulting in spectra similar to the liquid-state. MAS NMR has been used mainly for two classes of problems in structural biology, namely, for studying structures and interactions of membrane-bound peptides and for investigating conformations of ligands bound to large complexes.[4,18−21] The main advantage of this technique is the possibility to obtain well-resolved, solution-like spectra, which in combination with dipolar recoupling NMR yields spectral assignments and provides distance constraints and torsional angles.[22] However, obtaining orientational information from MAS data would require macroscopically ordered samples as shown for some studies on polymers or DNA fibers.[23,24] Therefore, we have recently suggested and demonstrated the application of MAS NMR to oriented membranes (MAOSS: magic angle oriented sample spinning NMR).[25] As shown in Figure 1, biomembranes can be uniformly aligned on thin glass disks[7,26] which are mounted into a MAS rotor so that the membrane normal is parallel to the rotor axis.[25] Whereas our previous work was mainly concentrated on mobile lipids, we describe here for the first time how MAOSS can be used for measuring orientations of molecular groups within immobile membrane proteins.

It is well-established that the broad characteristic powder spectrum of anisotropic interactions such as chemical shift or quadrupole coupling, decays under MAS conditions into a set of narrow, well-resolved spinning sidebands around the isotropic chemical shift central resonance, if the spinning speed does not exceed the anisotropy.[17] The intensity of each of these sidebands depends on the size of the interaction tensor, which can then be determined.[17,27,28] In a partially ordered system, such as uniformly aligned membranes, these sideband intensities feature an additional orientational dependence, which allows tensor orientations with respect to the sample director to be measured. The advantage of this approach is due to the distribution of spectral intensity (linebroadening) arising from disorder in the sample, which is refocused in narrow MAS resonance lines causing a significant improvement in resolution and sensitivity. This allows reliable data to be obtained from lower spin concentrations and even to resolve inequivalent sites. Resolution enhancement and retention of the isotropic chemical shift, while all orientational information is contained in the sideband intensities, could allow a spectral assignment which is of central importance for multiple labeling.

Any inhomogeneous NMR interaction such as chemical shift anisotropy or heteronuclear dipolar or quadrupole coupling could be used to demonstrate the applicability and usefulness of the suggested MAOSS approach. Here, as a straightforward demonstration of the approach, we have chosen the deuterium quadrupole coupling as an NMR interaction and the well-

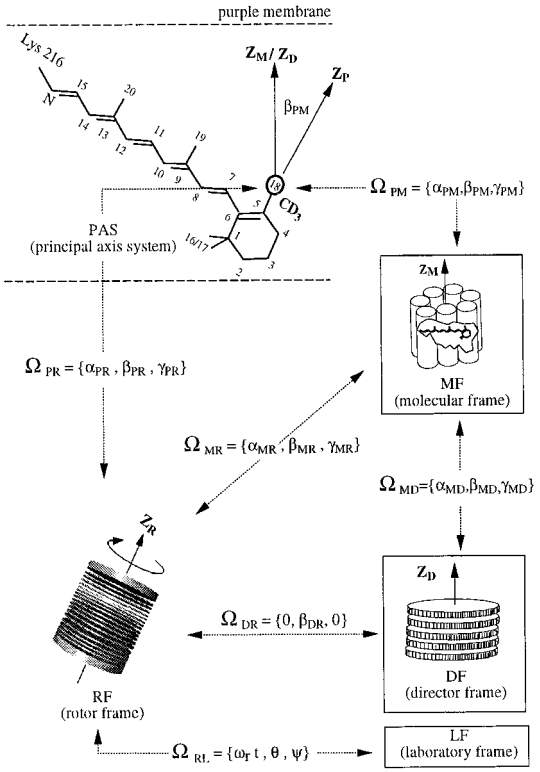

Figure 1. Method used to determine tilt angles for labeled groups by the MAOSS NMR method: Uniaxially oriented samples on glass disks are stacked in a MAS rotor, with rotor axis Z_R parallel to the sample director Z_D ($\beta_{DR} = 0°$). The protein long axis Z_M, defined as the average vector of all seven helix axes, is parallel to Z_D within a certain degree of disorder ($\beta_{MD} = 0° \pm \Delta\beta$). The principal axis system PAS of the EFG tensor of the deuterated methyl group has its largest component along the C−CD_3 bond (Z_P) and is related to MF by a set of unknown Euler angles Ω_{PM}. The MAS spectra obtained by this experimental setup are sensitive to Ω_{PR} and can be related to Ω_{PM} through coordinate transformations. The Euler angles are defined as rotation about *z*-axis through α ($0 \le \alpha \le 2\pi$), a rotation about the new y_1-axis through β ($0 \le \beta \le \pi$) and a rotation about the new z_2-axis through γ ($0 \le \gamma_{PL} \le 2\pi$).

(14) Ketchem, R. R.; Hu, W.; Cross, T. A. *Science* **1993**, *261*, 1457−1460.
(15) Bechinger, B.; Gierasch, L. M.; Montal, M.; Zasloff, M.; Opella, S. J. *Solid State NMR* **1996**, *7*, 185−191.
(16) Marassi, F. M.; Ramamoorthy, A.; Opella, S. J. *Proc. Natl. Acad. Sci. U.S.A.* **1997**, *94*, 8551−8556.
(17) Maricq, M. M.; Waugh, J. S. *J. Chem. Phys.* **1979**, *70*, 3300−3316.
(18) Spooner, P. J. R.; Rutherford, N. G.; Watts, A.; Henderson, P. J. F. *Proc. Natl. Acad. Sci. U.S.A.* **1994**, *91*, 3877−3881.
(19) Middleton, D. A.; Robins, R.; Feng, X. L.; Levitt, M. H.; Spiers, I. D.; Schwalbe, C. H.; Reid, D. G.; Watts, A. *FEBS Lett.* **1997**, *410*, 269−274.
(20) Williamson, P. T. F.; Gröbner, G.; Miller, K.; Watts, A. *Biochemistry* **1998**, *37*, 10854−10859.
(21) Feng, X.; Verdegem, P. J. E.; Lee, Y. K.; Sandstrom, D.; Eden, M.; BoveeGeurts, P.; de Grip, W. J.; Lugtenburg, J.; de Groot, H. J. M.; Levitt, M. H. *J. Am. Chem. Soc.* **1997**, *119*, 6853−6857.
(22) Griffin, R. G. *Nat. Struct. Biol. Suppl.* **1998**, *5*, 508−512.
(23) Song, Z. Y.; Antzutkin, O. N.; Lee, Y. K.; Shekar, S. C.; Rupprecht, A.; Levitt, M. H. *Biophys. J.* **1997**, *73*, 1539−1552.
(24) Schmidt-Rohr, K.; Spiess, H. W. *Multidimensional Solid-State NMR and Polymers*; Academic Press: London, 1994.
(25) Glaubitz, C.; Watts, A. *J. Magn. Res.* **1998**, *130*, 305−316.
(26) Smith, R.; Separovic, F.; Bennet, F. C.; Cornell, B. A. *Biophys. J.* **1992**, *63*, 469−474.
(27) Herzfeld, J.; Berger, A. E. *J. Chem. Phys.* **1980**, *73*, 6021.
(28) de Groot, H. J. M.; Smith, S. O.; Kolbert, A. C.; Courtin, J. M. L.; Winkel, C.; Lugtenburg, J.; Herzfeld, J.; Griffin, R. G. *J. Magn. Res.* **1991**, *91*, 30−38.

characterized membrane protein bacteriorhodopsin as a molecular system.

Bacteriorhodopsin (26 kD) is a light-driven proton pump from the archeobacterium *Halobacterium salinarium*.[29−31] The conformational change of the chromophore retinal in the protein, acting as a molecular "switch" upon light activation, is an ideal test case to visualize the sensitivity of the MAOSS NMR technique. We used *all-trans*-retinal with a deuterated methyl group at position C_{18} (see Figure 1) in bR in the ground state (bR_{568}) and upon light activation (M_{412}). The expected conformational change to 13-*cis*-retinal causes a different orientation of the C−CD_3 vector with respect to the membrane normal, which is directly reflected in experimental ^{2}H-MAOSS spectra. A theoretical description and the necessary data analysis are then applied and discussed below.

Theory

Orientational Dependence of ^{2}H-MAS Sidebands. The orientation of the principal axis system of the quadrupole interaction between the electric field gradient at the deuterium nucleus and its electric quadrupole moment is related to the relevant molecular and external reference frames by sets of Euler angles Ω[32] as shown in Figure 1. The fast rotation of the methyl group causes the unique *z*-axis Z_P of the PAS of the electric field gradient tensor to coincide with the C−C bond vector. The orientation of the axis Z_P with respect to the protein long axis Z_M is to be determined (β_{PM}). We define the *z*-axis Z_M of our molecular reference frame (MF) as the average vector of all seven protein helix long axes, which would be identical to the sample director Z_D in a perfectly aligned sample ($\beta_{MD} = 0°$). The sample director frame (DF) is identical in our experimental setup with the rotor fixed frame (RF), i.e., $Z_D \| Z_R$ ($\beta_{DR} = 0°$). The rotor frame axis Z_R is tilted with respect to the laboratory frame (LF) by the magic angle θ. Sample rotation makes a time-dependent set of Euler angles $\Omega_{RL}(\omega_r t,\theta,\psi)$ necessary.

First, an ideal situation is considered, where Z_M, Z_D, and Z_R are identical, parallel to B_0, and where no sample rotation is performed. The quadrupole Hamiltonian in the high-field approximation is given by[33]

$$H_Q = \frac{eQeq(3\mathbf{I}_z^2 - 2)}{4\hbar} \times \left(D_{00}^{(2)}(\Omega_{PL}) - \frac{\eta}{\sqrt{6}}(D_{-20}^{(2)}(\Omega_{PL}) + D_{20}^{(2)}(\Omega_{PL}))\right) \quad (1)$$

where $D_{qq'}^{(2)}$ are elements of Wigner rotation matrices, Q is the quadrupole moment, and eq is the principal value, V_{zz}^{PAS}, of the field gradient tensor. The asymmetry parameter η is defined as $(V_{yy} - V_{xx})/V_{zz}$, and Ω_{PL} are the Euler angles describing the rotation from the principal axis system PAS into the LF. The spectrum consists of two resonances ω^+ and ω^-, corresponding to both transitions of the quadrupole interaction.

$$\omega^{\pm} = \pm\delta_Q\left(\frac{3\cos^2\beta_{PL} - 1}{2} - \frac{\eta}{2}\sin^2\beta_{PL}\cos 2\alpha_{PL}\right) \quad (2)$$

The quadrupole coupling constant $\chi_Q = e^2qQ/\hbar$ is replaced by $^4/_3\delta_Q$. Under sample rotation, the Hamiltonian H_Q becomes time dependent,[34] and the Wigner matrix elements in eq 1 have to be modified by

$$D_{qq'}^{(2)}(\Omega_{PL}, t) = \sum_{i=-2}^{+2} D_{qi}^{(2)}(\Omega_{PR})\, D_{iq'}^{(2)}(\omega_r t + \varphi_0, \theta, \psi) \quad (3)$$

where Ω_{PR} are the Euler angles rotating the PAS into the RF, and $\Omega_{RL} = (\omega_r t + \varphi_0, \theta, \psi)$ describes the time-dependent rotation from the rotor frame into the laboratory frame. After some algebra $\omega^{\pm}(t)$ can be expressed as[17]

$$\omega^{\pm}(t) = \pm\delta_Q\left(\frac{3\cos^2\theta - 1}{2}\right)\left(\frac{3\cos^2\beta_{PR} - 1}{2} - \frac{\eta}{2}\sin^2\beta_{PR}\cos 2\alpha_{PR}\right) \pm \delta_Q\Psi(t) \quad (4)$$

where $\Psi(t)$ contains all time-dependent terms. The first term collapses under MAS conditions ($\cos\theta = 1/\sqrt{3}$), and the fast rotation of the deuterated methyl group about the C−C axis pre-averages the quadrupole interaction, so that δ_Q and η have to be replaced by their effective values. The asymmetry parameter η^{eff} is considerably small and can be safely set to zero, while δ_Q^{eff} is approximately one-third of the static coupling constant (∼39 kHz).[35] Thus, the expression above can be simplified to

$$\omega^{\pm}(t) = \pm\delta_Q^{eff}\Psi(t) \quad (5)$$

with $\Psi(t)$ given by

$$\Psi(t) = C_1\cos(\omega_r t) + C_2\cos(2\omega_r t) \quad (6)$$

$$C_1 = -^3/_4\sin 2\theta \sin 2\beta_{PR} \quad (7)$$

$$C_2 = +^3/_4\sin^2\theta \sin^2\beta_{PR}$$

The time domain signal of a single site in a crystallite can now be calculated as

$$S^{\pm}(t) = \exp[i\Phi^{\pm}(\beta_{PR}, t)] \quad (8)$$

where $\Phi^{\pm}(\beta_{PR}, t)$ is the phase angle describing the evolution of the magnetization vector under sample rotation

$$\Phi^{\pm}(\beta_{PR}) = \int_0^t \omega^{\pm}(\beta_{PR}, t')dt' \quad (9)$$

$$= \pm\frac{\delta_Q^{eff}}{\omega_r}\left(C_1\sin\omega_r t + \frac{1}{2}C_2\sin 2\omega_r t\right) - \Phi_0^{\pm}$$

The anisotropy is scaled with $1/\omega_r$, but for modest spinning speeds $\delta_Q/\omega_r \geq 1$, rotor echoes are observed in the time domain signal or sidebands separated by ω_r around the isotropic line in the NMR spectrum. Their intensities $I_N^{\pm}$ are obtained by Fourier transforming $S^{\pm}(t)$ over one rotor period. I_N is usually complex, giving rise to positive and negative sidebands.[17,33]

(29) Österhelt, D.; Stöckenius, W. *Proc. Natl. Acad. Sci. U.S.A.* **1973**, *70*, 2853−2857.
(30) Khorana, H. G. *Proc. Natl. Acad. Sci. U.S.A.* **1993**, *90*, 1166−1171.
(31) Henderson, R.; Baldwin, J. M.; Ceska, T. A.; Zemlin, F.; Beckmann, E.; Downing, K. H. *J. Mol. Biol.* **1990**, *213*, 899−929.
(32) Varshalovich, D. A.; Moskalev, A. N.; Khersonskii, V. K. *Quantum Theory of Angular Momentum*; World Scientific: Singapore, 1988.
(33) Mehring, M. *Principles of High Resolution NMR in Solids*; Academic Press, New York 1976.
(34) Haeberlen, U. *High Resolution in Solids: Selective Averaging*; Springer Verlag: Berlin, 1983.
(35) Seelig, J. *Q. Rev. Biophys.* **1977**, *10*, 345−418.

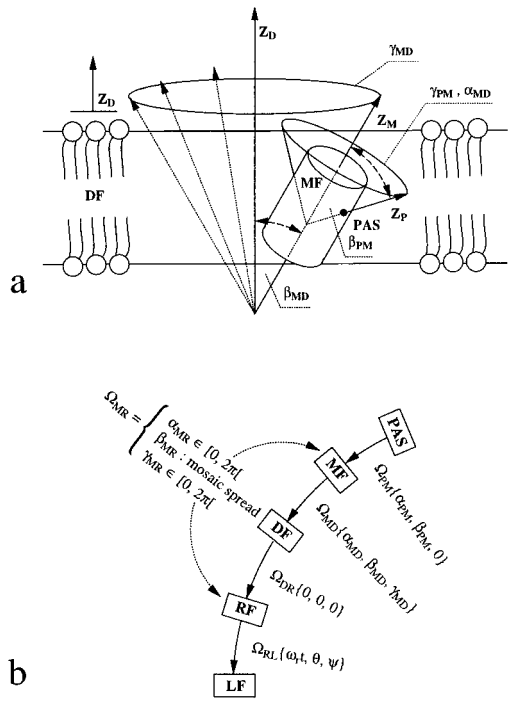

Figure 2. Distribution of molecular long axis Z_M and PAS (Z_P) shown around the sample director Z_D: Both distributions are uniaxial but not identical, but angles α_{MD} and γ_{PM} describe rotations about the same axis (a). Summary of rotations and averages required for simulating MAS spectra of NMR interaction for the special distribution in oriented membranes (b). All averaging steps can be shifted into the rotation MF → RF, since RF and the sample fixed frame DF are identical ($\Omega_{DR}(0, 0, 0)$).

However, in our experimental setup as shown in Figure 1, the *z*-axis Z_M of the molecular frame and the *z*-axis Z_P of the principal axis system are uniaxially distributed about the sample director Z_D and therefore about the rotor axis Z_R (see Figure 2a), which causes absorptive sidebands only[17,24] given by

$$I^{\pm}_N(\beta_{PR}) = |F^{\pm}_N(\beta_{PR})|^2 \tag{10}$$

with

$$F^{\pm}_N(\beta_{PR}) = \int_0^{2\pi} \frac{d(\omega_r t)}{2\pi} \exp\left[i\left(\frac{\delta^{eff}_Q}{\omega_r} \left(\pm C_1 \sin \omega_r t \pm \frac{1}{2} C_2 \sin 2\omega_r t \right) - N\omega_r t \right) \right] \tag{11}$$

Taking both quadrupole transitions into account, the total intensity of a sideband at position $N\omega_r$ is calculated by

$$I_N(\beta_{PR}) = I^{+}_N(\beta_{PR}) + I^{-}_N(\beta_{PR}) \tag{12}$$

Two special cases can now be discussed. If the C−CD_3 vector is oriented along the rotor axis Z_R, i.e., $\beta_{PR} = 0°$, both terms C_1 and C_2 (eq 7) will vanish. It can be easily seen from eq 11 that only the isotropic line ($N = 0$) remains and contains all signal intensity, which is not a surprise since the axially symmetric quadrupole interaction is now aligned at the magic angle. If the bond vector now takes a perpendicular orientation to Z_R, i.e., $\beta_{PR} = 90°$, only the term C_1 vanishes, leaving a ($2\omega_r t$) periodicity in $F_N^{\pm}(\beta_{PR})$, while the ($\omega_r t$) periodicity vanishes. This means that spectral intensity is only observed at even numbered sidebands ($N = 0,2,4...$), while at odd numbers no signal appears.

Distribution and Disorder in Oriented Samples. The principal axis system of the quadrupole interaction is rotated into the MF by Ω_{PM}, from there into the DF by Ω_{MD} and finally into RF by Ω_{DR}. The Wigner rotation matrix elements $D^{(2)}_{qi}(\Omega_{PR})$ in eq 3 have to be replaced by

$$D^{(2)}_{qi}(\Omega_{PR}) = \sum_{j=-2}^{+2} \sum_{k=-2}^{+2} D^{(2)}_{qk}(\Omega_{PM}) D^{(2)}_{kj}(\Omega_{MD}) D^{(2)}_{ji}(\Omega_{DR}) \tag{13}$$

Since DF is identical to RF, all rotations below will now refer directly to the rotor frame rather than to the sample fixed coordinate system and the expression above simplifies to

$$D^{(2)}_{qi}(\Omega_{PR}) = \sum_{j=-2}^{+2} D^{(2)}_{qj}(\Omega_{PM}) D^{(2)}_{ji}(\Omega_{MR}) \tag{14}$$

Because both coordinate systems, PAS and MF, are uniaxially distributed about the director normal Z_D and so about the rotor axis Z_R, as illustrated in Figure 2a, the expression for I_N has to be averaged over γ_{PM} and γ_{MD}. However, the angles γ_{PM} and α_{MD} describe rotations about the same axis Z_M, which is the final *z*-axis while rotating from PAS to MF and at the same time the initial *z*-axis for the rotation from MF to DF. Finally, only one rotation about Z_M by an angle $\gamma_{PM} + \alpha_{MD}$ takes place, which allows the elimination of one averaging step by choosing either $\gamma_{PM} = 0$ or $\alpha_{MD} = 0$. Here, $\gamma_{PM} = 0$ will be used. To account for the two uniaxial distributions of PAS and MF, the correct sideband intensity I_N is obtained from

$$I_N(\beta_{PM}, \beta_{MR}) = \int_0^{2\pi} \frac{d\alpha_{MR}}{2\pi} \int_0^{2\pi} \frac{d\gamma_{MR}}{2\pi} I_N((0, \beta_{PM}, 0), (\alpha_{MR}, \beta_{MR}, \gamma_{MR})) \tag{15}$$

Additionally, a certain distribution of the molecular long axis Z_M with respect to the sample director Z_D has to be assumed. The degree of disorder ("mosaic spread" $\Delta\beta$), is best described by a Gaussian probability distribution of β_{MR} around 0° with a weighting factor of sin β_{MR}[12]

$$p_{MR}(\beta_{MR}) = M \int_0^{\beta_{MR}} \exp\left[-\frac{1}{2}\left(\frac{\beta}{\Delta\beta} \right)^2 \right] \sin\beta \, d\beta \tag{16}$$

where M is a normalization constant. The intensity of a MAS sideband is now a function of two Euler angles describing the tilt of the C−CD_3 bond axis with respect to the protein axis Z_M, and the width of the distribution of Z_M

$$I_N(\beta_{PM}, \Delta\beta) = K \int_0^{2\pi} d\alpha_{MR} \int_0^{2\pi} d\gamma_{MR} \int_{-\Delta\beta}^{+\Delta\beta} d\beta_{MR} \times p_{MR}(\beta_{MR}) I_N((0, \beta_{PM}, 0), (\alpha_{MR}, \beta_{MR}, \gamma_{MR})) \tag{17}$$

with K being an integration constant. A summary of all necessary frame rotations and averagings is shown in Figure 2b and the dependence of the ^{2}H-MAS sideband pattern on the tilt angle β_{PM} in a well-oriented system ($\Delta\beta = 0°$) is shown in Figure 3a for a relative spinning speed $\kappa = \omega_r/\chi_Q$. As discussed before, for $\beta_{PM} = 0°$, only the isotropic central resonance remains, while for $\beta_{PM} = 90°$ all odd-numbered sidebands vanish. C−CD_3 bond vector orientations can now be determined by fitting these simulated sideband patterns to experimental MAOSS spectra. The effect which different degrees of disorder ($\Delta\beta$) would have on a spectrum corresponding to a particular orientation is shown in Figure 3b. A tilt angle of $\beta_{PM} = 0°$ was chosen because MAOSS spectra are particularly sensitive to

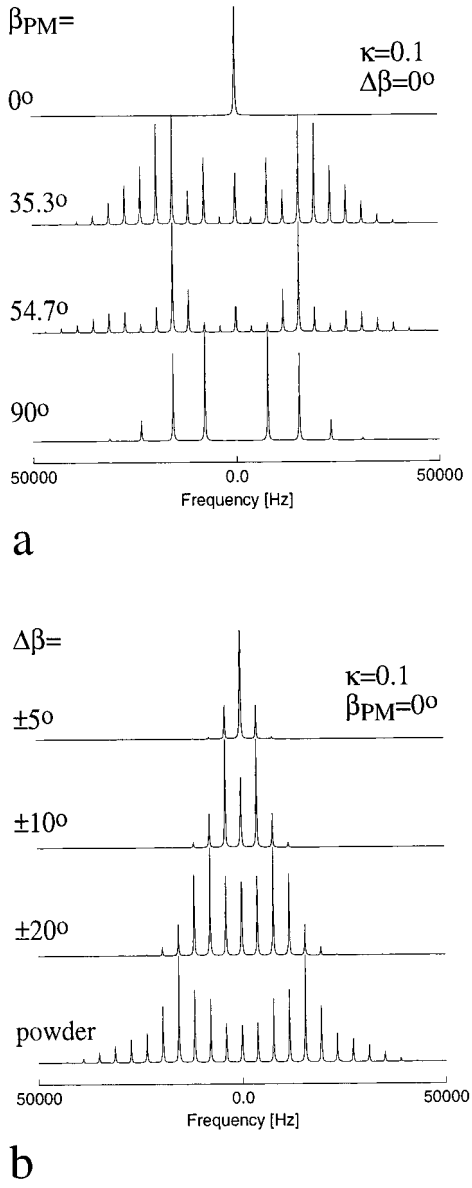

Figure 3. Simulations of ^{2}H MAS spectra for different tilt angles β_{PM} of the C−CD_3 vector with respect to the molecular frame in a perfectly aligned sample ($\Delta\beta = \pm 0°$) (a), and for the particular vector orientation of $\beta_{PM} = 0°$ with different degrees of disorder $\Delta\beta$ (b). The relative spinning speed κ is the ratio of ω_r and quadrupole coupling.

deviations from 0°. It can be seen that the intensities of the narrow MAS sidebands are changing, while without sample spinning, a severe linebroadening would be observed.

A realistic situation is shown in Figure 4. Spectra were simulated for different orientations θ of the sample director frame assuming a tilt angle of $\beta_{PM} = 35.3°$ and a mosaic spread of $\Delta\beta = 10°$. While in principle the tensor orientation can be obtained from the static oriented spectra by using eq 2, difficulties are encountered due to the low spectral resolution and sensitivity. An essential sensitivity and resolution improvement is achieved under MAS conditions, as shown for two relative spinning speeds κ.

Since the description above can be easily generalized for other applications, it should be pointed out that the distributions of Ω_{MD} and Ω_{DR} are statistically independent in our experimental setup, which is, however, not necessarily the case for other ordered systems, such as DNA fibers, where the macroscopic order Ω_{DR} is coupled to the microscopic order Ω_{MD}.[23]

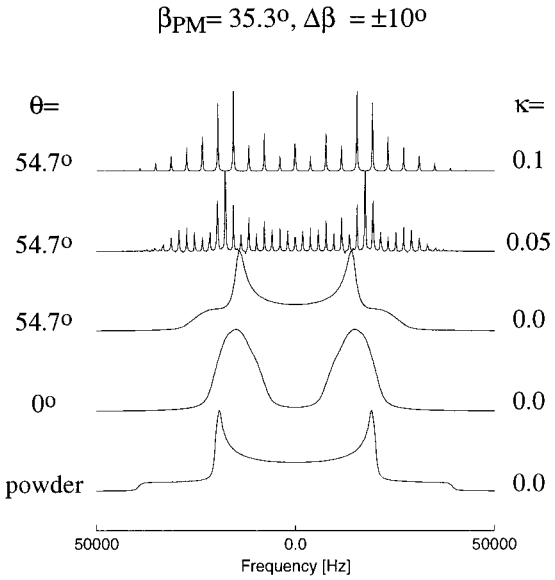

Figure 4. Comparison between static and MAS NMR on oriented membranes (MAOSS) for the case of a C−CD_3 vector tilt angle of $\beta_{PM} = 35.3°$ and a degree of disorder of $\Delta\beta = \pm 10°$. The lineshape becomes more complex while tilting the membrane normal with respect to B_0 from $\theta = 0°$ to 54.7°. Additional sample spinning is refocussing all signal intensity in narrow spinning sidebands.

Materials and Methods

Sample Preparation. *All-trans*-retinal was synthesized following the procedures of Groesbeek[36] and specifically deuterated on the methyl group at the C_{18} position following the method of Pardoen.[37] The retinal was regenerated into retinal-deficient bacteriorhodopsin, according to published procedures.[38] Purple membrane was isolated according to the method of Österhelt and Stöckenius.[39] On average 12 mg of bacteriorhodopsin was obtained per liter of culture.

Sample Orientation. Purified purple membrane was washed repeatedly in deuterium-depleted water and spread evenly (0.2 mg protein in 25 μL H_2O) over 80, round, 0.07-mm thin glass disks with a diameter of 5.4 mm (Marienfelde GmbH, Germany). Uniaxial films with good orientation of the purple membrane patches parallel to the sample director were produced by controlled evaporation of the bulk water at 85% relative air humidity and 4 °C over a period 48 h. A second application produced a final concentration of 0.4 mg protein per plate. The optimum between maximal protein concentration and best orientation was checked by polarized light microscopy.[40] The glass plates had previously been cleaned in nitric acid and methanol/ethanol and dried under a stream of nitrogen gas. Finally, all 60 disks (24 mg bR) were placed on top of each other and mounted into a MAS rotor using specifically designed tools and special KelF inserts.

Sample orientation and stability was monitored by static ^{31}P NMR before and after the MAS experiments. No changes in the spectral lineshape were detected. The mosaic spread $\Delta\beta$ was typically between ±5° and ±10°. Additionally, oriented bR samples on glass disks were studied by light microscopy before and after sample rotation to verify their stability. An unoriented sample containing 25 mg bR was prepared by transferring a membrane pellet into a MAS rotor.

Trapping bR in the M_{412} state. Disks with oriented bR were hydrated in 0.3 M guanidine hydrochloride pH 10 for 2 h and then returned to 85% humidity for a further 12 h. The disks were then mounted one by one on a precooled stacking tool (−60 °C) under strong illumination. A purple to yellow/orange colour change was observed. The disks were mounted and kept in a 7 mm rotor at −60 °C.

(36) Groesbeck, M. Ph.D. Thesis, University of Leiden, Leiden, 1993.
(37) Pardoen, J. A. Ph.D. Thesis, University of Leiden, Leiden, 1986.
(38) Österhelt, D. *Methods Enzymol.* **1982**, *88*, 11−17.
(39) Österhelt, D.; Stöckenius, W. *Methods Enzymol.* **1974**, *31*, 667−678.
(40) Asher, S. A.; Pershan, P. S. *Biophys. J.* **1979**, *27*, 393−421.

NMR Experiments. All NMR experiments were performed at 61.402 MHz on a BRUKER MSL 400 and a double resonance 7 mm MAS probe. NMR spectra were recorded using a "single pulse" sequence with the sample subject to MAS and without high power proton decoupling. A $\pi/2$ pulse was typically 6 μs. The spinning rate was stabilized within a range of ± 3 Hz. Experiments were performed at 210 K and 4040 Hz spinning speed. Between 100 000 and 400 000 scans were acquired with a recycle delay time of 300 ms. Spectra were zerofilled with 16k points, Fourier-transformed, and carefully phase-corrected. An exponential linebroadening of 50 Hz was applied. Finally, spectra were symmetrized to account for some remaining asymmetry due to the amplifier in use.

Simulation Software. A program for MAS lineshape simulations of oriented systems was written using the NMR software library GAMMA-3.5b.[41] The MAS Hamiltonian was calculated by using Floquet theory[42] with a Floquet space truncated to a dimension of 15. Spinning sideband patterns of a single spin-$^1/_2$ or spin-1 can be calculated for various distributions, from a single crystal to the full powder. This is achieved by defining explicitly the range of the Euler angles, which define the orientation of the PAS with respect to the molecular frame (Ω_{PM}) and the orientation of the molecular frame to the rotor fixed system (Ω_{MR}). The Monte Carlo method is applied for sampling over these defined intervals, and an appropriate weighting function is applied. All simulations were performed on a Silicon Graphics INDY R4600 workstation. Between 30 s and 10 min CPU time are required for each spectrum.

Results and Data Analysis

^{2}H MAOSS spectra of [18-CD_3]-retinal in the ground state bR_{568} and the photo intermediate state M_{412} are shown in Figure 5a and 5b. Both spectra were acquired at $T = 210$ K and $\omega_r = 4040$ Hz and show a significant difference in the intensity distribution in the spinning sideband pattern, which is due to the conformational change from all-*trans*- into 13-*cis*-retinal upon photoactivation. The central resonance $N = 0$, which is the isotropic chemical shift of CD_3, is surrounded by spinning sidebands of different intensities, each a function of β_{PM}, $\Delta\beta$, ω_r, N, and χ_Q^{eff} (eq 17). The linewidth at half height is found to be ± 90 Hz. The analysis of ^{2}H MAS spectra of unoriented bR reveals a quadrupole coupling constant of 39 kHz, which is identical to published values for the CD_3 rotor.[43] The degree of disorder $\Delta\beta$ can be estimated indirectly from the disorder of lipids by analyzing ^{31}P spectra and is used as a restricted fitting parameter. In order to analyze the obtained spectra, a χ^2 merit function

$$\chi^2(\beta_{PM}, \Delta\beta) = \sum_N \left(\frac{I_N^{ex} - I_N^{sim}(\beta_{PM}, \Delta\beta)}{\Delta I_N^{ex}} \right)^2 \qquad (18)$$

has been minimized for the tilt angle β_{PM} and mosaic spread $\Delta\beta$, with I_N^{ex} and I_N^{sim} being experimental and simulated spectral intensities. The rms noise amplitude is used as an experimental error ΔI_N^{ex} with which a sideband intensity can be measured and has been determined to be $\sim$10% of the maximum intensity. The χ^2 plot for bR_{568}, as shown in Figure 5c, reveals a global minimum at $\beta_{PM} = 36°$ and a mosaic spread $\Delta\beta$ between $\pm 0°$ and $\pm 8°$. The function for χ^2 was minimized for different values $\Delta\beta$, which are in the range of experimentally estimated disorder. It is found that the global minimum is broadened by increasing the degree of disorder in the system (Figure 5c). The best fit spectrum for bR_{568} is compared with the experimental spectrum in Figure 5a.

The same procedure was applied to the data obtained in the M_{412} photo intermediate state, which yields a tilt angle of the Z_P axis to Z_M of $\beta_{PM} = 22°$ with $\Delta\beta$ between $\pm 10°$ and $\pm 18°$. However, a careful analysis shows that some remaining contributions from bR_{568} are contained in the observed signal. This is found by minimizing χ^2 simultaneously over β_{PM} and $\beta_{PM}^{bR_{568}} + k\beta_{PM}$. The χ^2 slice for $\beta_{PM} = 22°$ in Figure 5d shows that two populations, 70% M_{412} and 30% bR_{568}, were observed. The best fit spectrum taking this into account is plotted in Figure 5b.

It is important to identify potential sources of error and to quantify the uncertainties of the fitting parameters when introducing new methodology. The only free parameter is β_{PM} for which an error has to be estimated, which is difficult to do directly, since β_{PM} modulates the sideband intensities in a nonlinear way (eq 17). However, by performing χ^2 minimizations on synthetic MAOSS spectra, which were randomly altered by the potential error sources using the Monte Carlo method, an estimated error can be given.[44]

Gaussian noise was added to a set of simulated spectra in order to investigate the effect of the experimentally observed signal-to-noise. A χ^2 minimization was performed, which gave a width of $\pm 2°$ for the distribution of the best fit value of β_{PM}. Furthermore, the deuterium natural abundance of 0.015% would result in a 2$-$3% contribution to the signal from the CD_3 label. The effect of natural abundance background was simulated by randomly varying individual sideband intensities at constant signal-to-noise, which gave an uncertainty of $\pm 0.5-1°$.

Another error source is the quality of orientation in the sample. It is shown in Figure 5c that the χ^2 minimum gets broader with increasing mosaic spread, for which MC simulations yield an additional error of $\pm 2°$ for a mosaic spread of $\Delta\beta = \pm 8°$. As expected, it can be concluded that the experimental error for determining the tilt angle β_{PM} increases with decreasing signal-to-noise, decreasing spin concentration, and increasing disorder.

Additionally, the precision of the quadrupole coupling constant and the asymmetry parameter are of importance. A variation of ± 1 kHz in the quadrupole coupling constant would cause an angle variation of $\pm 1°$. However, both parameters can be determined to a high precision. Therefore, the angles obtained for bR_{568} and M_{412} have to be considered with a maximal error of $\Delta\beta_{PM} = \pm 5°$.

The remaining small discrepancies between experimental and simulated MAOSS spectra in Figure 5a and 5b could be from small populations of other photointermediates of bR or from dynamic effects, which were not included in the data analysis.

Discussion

Bacteriorhodopsin is an attractive molecular test system, since it is well-characterized and the orientation of the retinal in the ground state has been measured previously. This allows a direct comparison of results obtained by different methods such as X-ray diffraction, electron microscopy, and static ^{2}H NMR.[12,45−47]

(41) Smith, S. A.; Levante, T. O.; Meier, B. H.; Ernst, R. R. *J. Magn. Res. A.* **1994**, *106*, 75−105.
(42) Baldus, M.; Levante, T. O.; Meier, B. H. *Z. Naturforsch., A: Phys. Sci.* **1993**, *49a*, 80−88.
(43) Copie, V.; McDermott, A.; Beshah, K.; Williams, J. C.; Spijker-Assink, M.; Gebhard, R.; Lugtenburg, J.; Hertzfeld, J.; Griffin, R. G. *Biochemistry* **1994**, *33*, 3280−3286.
(44) Press, W. H.; Teukolsky, S. A.; Vetterling, W. A.; Flannery, B. P. *Numerical Recipes*; Cambridge University Press: New York, 1992.
(45) Ulrich, A. S.; Watts, A.; Wallat, I.; Heyn, M. P. *Biochemistry* **1994**, *33*, 5370−5375.
(46) Pebay-Peyroula, E.; Rummel, G.; Rosenbusch, J. P.; Landau, E. M. *Science* **1997**, *277*, 1676−1681.
(47) Grigorieff, N.; Ceska, T. A.; Downing, K. H.; Baldwin, J. M.; Henderson, R. *J. Mol. Biol.* **1996**, *259*, 393−421.

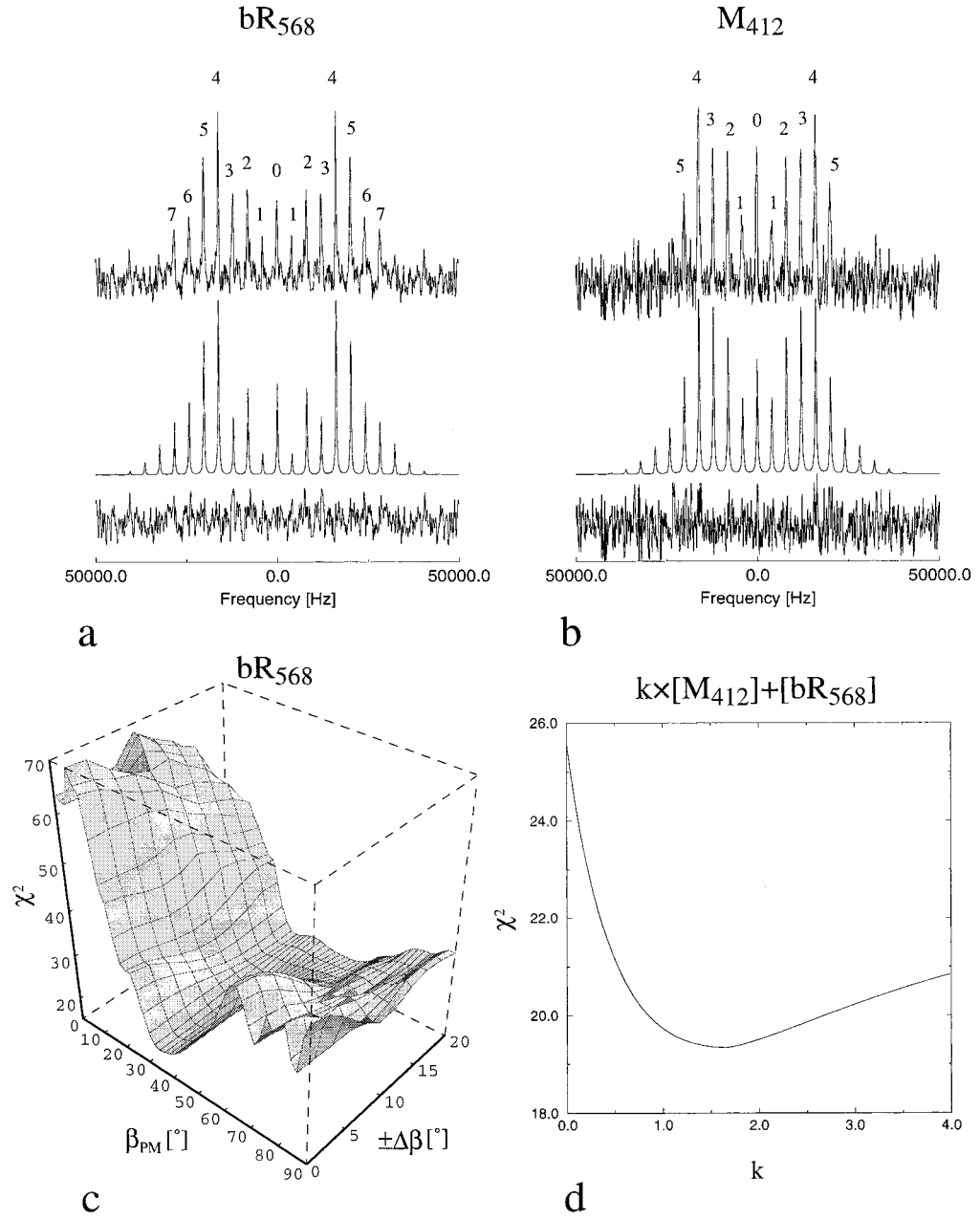

Figure 5. Comparison between experimental ^{2}H MAOSS spectrum of bR in the ground state (bR_{568}), best-fit simulation, and the difference between them (a) and the respective spectra for the photo intermediate state M_{412} (b). Both experimental spectra were acquired at $T = 210$ K and $\omega_r = 4040$ Hz. The χ^2 plot for bR_{568} illustrates the best fit to be obtained for $\beta_{PM} = 36°$ (c). The same analysis applied to M_{412} gives a tilt angle of $\beta_{PM} = 22°$ but shows some remaining contributions from bR_{568} as well, so that the best fit is actually obtained for a spectrum consisting of ca. 70% M_{412} contributions (22°) and 30% bR_{568} (36°) (b),(d).

There is general agreement in the interpretation of these data that the structure of retinal in bR is distorted. The angle $\beta_{PM} = 36° \pm 5°$ for bR_{568} is in excellent agreement with the results from the static wideline NMR experiments, which were obtained under similar experimental conditions.[45] The tilt of the retinal ring of $\beta_{PM} = 22° \pm 5°$ upon photoactivation in M_{412} has never been measured before and reflects clearly the conformational change from all-*trans*- to 13-*cis*-retinal. However, an interpretation of our data in terms of a molecular model is beyond the scope of this paper and will be reported elsewhere. Here we show that resolution and sensitivity are greatly improved in the MAOSS experiment of ^{2}H-retinal in bR. The observed intrinsic linewidth in static NMR was in the order of 1−2 kHz,[12,45] and 2−3 kHz exponential linebroadening was usually applied compared to 180 Hz and 50 Hz in our case. The resolution is good enough to clearly observe a shift of the central MAS resonance line with respect to D_2O, corresponding to the chemical shift of CD_3.

Besides resolution and sensitivity, a further problem of static deuterium solid-state NMR for structure determination has been the spectral symmetry due to the spin-1 character of deuterons. If $35.3° \leq \beta_{PL} \leq 90°$ in eq 2 ($\eta = 0$), the observed quadrupole splitting $\Delta\omega = 2|\omega^{\pm}|$ can be related to two different angles. This ambiguity had been resolved in previous work by a series of spectra at different tilt angles θ, which is a time consuming approach, considering low sensitivity and resolution of these static spectra.[12,48] However, this problem does not occur in the MAS approach presented here. Each sideband intensity I_N is an orientational dependent function (eq 17), so that a spectrum with more than three sidebands presents an already overdetermined solution for the angle ambiguity. The correct orientation

(48) Ulrich, A. S.; Watts, A. *Solid State NMR* **1993**, *2*, 21−36.

is found as a global minimum in the χ^2 plot as shown in Figure 5c. It should be noted that the angle ambiguity in eq 2 is being modulated under MAS conditions (eqs 3,14) and is so reflected as local minima in Figure 5c. It can be shown that these local minima depend on the spinning speed ω_r in contrast to the global solution representing the correct orientation.[49] This means that an additional constraint to resolve potential orientational ambiguities could be found by recording spectra at different spinning speeds.

Our findings imply significant advantages of ^{2}H MAOSS over previously used wide-line methods. The improvement in sensitivity allows reliable data from lower spin concentrations to be obtained, for example from very large membrane proteins or from systems which can only be provided in limited quantities. Disorder does not cause severe linebroadening as in static NMR, but contributes to the intensity distribution of narrow MAS sidebands, so that well-resolved spectra can always be obtained, which is essential for multiple labeling. The use of multiple labels is also supported by the fact that the MAS central line is identical with the isotropic chemical shift ω_{CS}, which allows separation and identification of the signal from different sites, while all orientational information is contained in spinning sidebands appearing at $\pm N\omega_r$ around ω_{CS}. This might be only of limited use for deuterium application, for example, by using a 2D quadshift experiment,[50] since the dominating quadrupole coupling is usually much larger than the chemical shift distributions, but a clear potential is in the use of multiple ^{15}N and ^{13}C labels.

It should be noted that we present here the first application of ^{2}H MAS to a membrane protein at all, which is surprising, since even in unoriented systems essential information could be obtained more easily, compared to the static wideline approach. Lineshapes of deuteron-wideline spectra are highly sensitive to molecular order and the type and time scale of molecular motions, a property which has been used extensively for studying biomembranes.[35] Questions about lipid and protein dynamics,[51,52] lipid−protein interaction,[53,54] and membrane protein structures[11,55] have been addressed using deuterons. It has been suggested that ^{2}H MAS would actually extend the accessible range of dynamic processes remarkably and provides thereby a potentially useful method for investigating very fast and very slow molecular motions.[56]

Conclusions

We have shown that introducing a macroscopic anisotropy into membrane protein samples, which are usually studied as isotropic dispersion by MAS NMR, allows molecular orientations to be determined, which are otherwise difficult to obtain. These structural data are crucial for the elucidation of the mechanism of action of membrane proteins. The necessary macroscopic order is achieved in a mechanical way, but could be obtained in principle by choosing molecular systems which rearrange themselves under the influence of sample rotation and magnetic fields.[57]

Here it has been demonstrated that light-induced switching of the orientation of the 18-CD_3 bond vector in all-*trans*- and 13-*cis*-retinal in bR_{568} and M_{412} modulates the observed MAS sideband pattern in a highly sensitive manner, which can be analyzed reliably and precisely in a quantitative way. An efficient and unambiguous data analysis is possible due to the properties of the spinning sideband intensity function I_N. Further ^{2}H MAOSS experiments on bR_{568} and M_{412} have been performed with differently labeled retinal in order to establish a molecular model for the light-activated chromophore. Findings will be reported elsewhere.

The significant resolution and sensitivity enhancement achieved makes ^{2}H MAOSS a valuable tool for obtaining precise structural information in cases of low deuterium concentration. This is especially attractive for studying labeled groups in membrane proteins, which are not as easily available as bR (the deuterium concentration used here was only 3 μM).

The general MAOSS approach demonstrated here for the retinal chromophore in bacteriorhodopsin can be applied to two classes of problems. First, it can be used to investigate molecular orientation and conformation of ligands bound to membrane proteins, and second, orientation distribution functions of secondary structural elements within the anisotropic membrane environment can be determined. Various studies including multiple labeling strategies are currently in progress.

Acknowledgment. M. H. Levitt and M. Helmle are acknowledged for comments to the manuscript, J. M. Werner for advice on the statistical error analysis, and P. Spooner and B. Bonev for discussions. This work was supported by BBSRC (43/B04750), EU (TMR contract No. FMRX-CT96-0004), and the Rhodes Trust, Oxford (Scholarship for C.G.).

JA990350P

(49) Glaubitz, C. *Magic Angle Sample Spinning NMR Spectroscopy on Biomembranes*; D.Phil Thesis, University of Oxford, 1998.

(50) Chandrakumar, N.; Von Fircks, G.; Gunther, H. *Magn. Res. Chem.* **1994**, *32*, 433−435.

(51) Weisz, K.; Gröbner, G.; Mayer, C.; Stohrer, J.; Kothe, G. *Biochemistry* **1992**, *31*, 1100−1112.

(52) Prosser, R. S.; Daleman, S. I.; Davis, J. H. *Biophys. J.* **1994**, *66*, 1415−1428.

(53) Prosser, R. S.; Davis, J. H.; Mayer, C.; Weisz, K.; Kothe, G. *Biochemistry* **1992**, *31*, 9355−9363.

(54) Watts, A. *Magnetic Resonance Studies of Phospholipid-Protein Interactions in Bilayers*; Marcel Dekker: New York, 1993; pp 687−740.

(55) Prosser R. S.; Davis, J. H. *Biophys. J.* **1994**, *66*, 1429−1440.

(56) Kristensen, J. H.; Bildsoe, H.; Jakobsen, H. J.; Nielsen, N. C. *J. Magn. Res.* **1992**, *100*, 437−443.

(57) Courtieu, J., Bayle, J. P.; Fung, B. M. *Prog. Nucl. Magn. Reson. Spectrosc.* **1994**, *26*, 141−169.